A Statistical Characterization of the Atmospheres of Kepler's Planet Candidates

Holly Sheets[1,2] and Drake Deming[1,2]
[1]University of Maryland, College Park
[2]NASA Astrobiology Institute's Virtual Planetary Laboratory

Abstract: We present a method to detect small atmospheric signals in Kepler's planet candidate light curves by transforming and averaging light curves for multiple candidates with similar orbital and physical characteristics. This statistical method greatly increases the signal to noise, allowing for very small signals to be detected. We are looking for reflected light and/or thermal emission at secondary eclipse of planets significantly smaller than hot Jupiters. We also apply a similar method to search for signatures of light refracted by the planetary atmospheres just outside of transit.

Introduction:

Secondary eclipses have been detected in *Kepler* data for hot Jupiters (e.g. Coughlin and López-Morales 2012), showing that these bodies have very low albedos, as predicted by atmospheric models. For Super-Earth-sized planets, eclipses have only been detected with *Kepler* in the two extremely hot, close-in planets Kepler-10b (Batalha et al. 2011) and Kepler-78b (Sanchis-Ojeda et al. 2013). Unlike the hot Jupiters, these two planets show relatively high albedos, between 0.4 and 0.6. These planets are unlikely to harbor atmospheres at such extreme temperatures (> 1500 K). The *Kepler* data set contains many Super-Earths and sub-Saturn-sized candidates at slightly less extreme temperatures. At slightly lower temperatures and greater distances from the host star, the eclipse signals from these candidates are much weaker. We average the light curves of these candidates to increase the signal to noise and to gauge the average albedos of close-in Super-Earths and sub-Saturns, to see if their atmospheres are dark like those of the hot Jupiters. Averaging the light curves of multiple candidates can also be useful in looking for the small predicted signals (e.g. Sidis and Sari 2010) from refraction of light through the atmospheres of planets just before and after transit. We focus on objects between 1 and 6 Earth radii.

Data:

We use the short-cadence (~60 s exposure) PDC data from MAST, for quarters 0 through 15. We normalize each light curve by the mean flux outside of transit. We normalize again by cutting out each eclipse (at phase = 0.5, assuming circular orbits), including +/- 3 durations of the eclipse (based on the transit duration) and fitting a line across the out-of-eclipse section and dividing by the linear fit. We use a 3-sigma clip to exclude unusually high or low points. We also test each eclipse for discontinuities across the eclipse, due to instrumental effects, as well as differing slopes across each side of the eclipse, which would suggest that the star is too variable to use a simple linear fit across the eclipse. We reject noisy stars by calculating the standard deviation of the light curve when binned by 3, 5, 7, 9, 11, 13, and 15 points. Random noise, like photon-counting, should follow a log(σ) α -0.5*log(N) relation. For each individual eclipse, we fit a line to log(σ) versus log(N). We expect the distribution of the slope of this fit to be a Gaussian distribution around -0.5, if the noise in the eclipses is random noise. We exclude eclipses with slopes where the distribution deviates from the Gaussian expectation, typically above a slope of -0.3.

Adding Multiple Candidates:

To constructively add the eclipses of multiple objects, we take one candidate from the group being averaged to serve as the reference object. Then we transform the phase of all other objects in the group by scaling sections of the light curve to the reference object. Thus ingress, egress, and full eclipse all have the same duration in phase for all objects in the transformed phase coordinate. We then bin the normalized flux data using this transformed phase coordinate and take the average of the points in each bin, weighted by their photometric errors.

Results:

We select candidates that are between 1 and 6 Earth radii and split them into two lists. The first list is comprised of 33 candidates with $(R_p/a)^2 > 10$ ppm, which makes them more likely to be detectable even with low albedo. The second list of 516 candidates is the control list, with $(R_p/a)^2 < 1$ ppm, which makes them undetectable.

Figure 1 shows the result for the list of objects with $(R_p/a)^2 > 10$ ppm, containing 6850 individual eclipses. To test the significance of the dip at phase = 0.5, we fit a top-hat function to the data, fixing the width of the top-hat to the expected duration of the eclipse, and calculate the χ^2, moving the center of the top-hat function across in phase. Figure 2 shows the χ^2 values, with the best fit being centered at phase = 0.5. Also included in Figure 1 is the expected depth of the eclipse calculated from the reflected light + thermal emission for a range of albedos, adopting $A_{geometric} = A_{Bond}$. The dashed lines assume complete redistribution of heat across the planet, while the solid lines assume instantaneous re-radiation. Error bars on the eclipse depth are calculated by taking a weighted average of the binned points within eclipse and propagating the uncertainties. We find an eclipse depth of 5.0 +/- 0.5 ppm, consistent with an albedo of about 0.3. This group, however, includes two objects that have detectable eclipses on their own: Kepler-10b (Batalha et al 2011) and Kepler-4b (see poster 2-107). Removing these two objects from the average results in a smaller eclipse depth of 2.4 +/- 0.8 ppm, and the χ^2 significance is not as strong. The averaged light curve for the group, minus these two objects, contains 5693 individual eclipses and is shown in Figure 3.

Figure 4 shows the averaged light curve, containing 9978 individual eclipses, for the control group of objects with $(R_p/a)^2 < 1$ ppm. The best fit suggests an eclipse depth of 0.4 +/- 0.2 ppm, which is consistent with no detection.

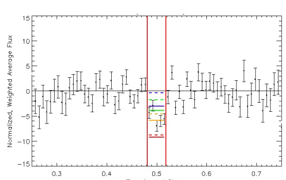

Figure 1: Averaged eclipse light curve for objects between 1 and 6 Earth radii, with $(R_p/a)^2 > 10$ ppm. The red vertical lines mark 2nd and 3rd contact. The dashed (full redistribution) and solid (instantaneous re-radiation) horizontal lines are the expected eclipse depths for $A_g = A_B = 0$ (blue), 0.1 (green), 0.3 (orange), and 0.6 (red).

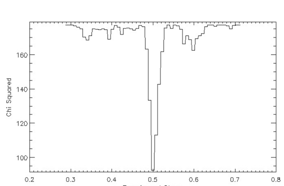

Figure 2: The χ^2 for fitting a top-hat with width equal to the duration of the eclipse to the data in Figure 1, as a function of the center of the top-hat.

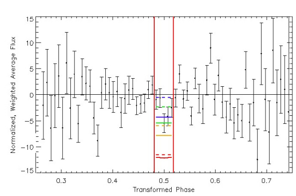

Figure 3: The same as Figure 1, only now excluding Kepler-4b and Kepler-10b from the list.

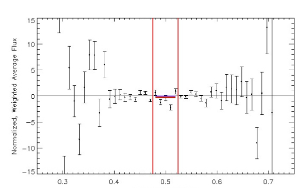

Figure 4: The control list of objects, with $(R_p/a)^2 < 1$ ppm. As expected, the eclipse depth is very small, with the detection of 0.4 +/- 0.2, consistent with no detection.

Future Work:

We shall continue working to understand the sources of noise in our averages, so that we can look for still smaller signals. We will also apply this method to the long cadence data, which drastically increases the available number of candidates to include in the averages. Lastly, Figure 5 shows preliminary results on our search for refracted light from planet atmospheres just outside of transit. The averaged light curve uses short cadence data for objects 2 to 3 Earth radii in size, with a predicted effect from Sidis & Sari's (2010) equations of 40 ppm or more. The green line is the averaged predicted effect from Sidis and Sari, while the blue line is with no refraction effect. The shoulders on the transit predicted from the Sidis and Sari model are clearly not present.

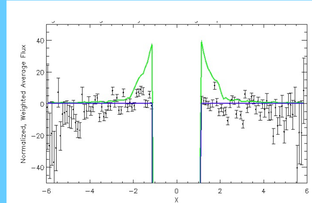

Figure 5: Averaged transit light curve for objects between 2 and 3 Earth radii. Over-plotted in green is the predicted refraction effect from the Sidis and Sari (2010) model, while over-plotted in blue is the expectation with no refraction effect. This curve is plotted versus X, which is the projected distance on the sky between the planet center and host star center, rather than phase.

References:

Batalha, N. M., Borucki, W. J., Bryson, S. T., et al. 2011, ApJ, 729, 27
Coughlin, J. L., & López-Morales, M. 2012, AJ, 143, 39
Sanchis-Ojeda, R., Rappaport, S., Winn, J. N., et al. 2013, ApJ, 774, 54
Sidis, O., & Sari, R. 2010, ApJ, 720, 904